

Light Scalar Meson $\sigma(600)$ in QCD Sum Rule with Continuum

Hua-Xing Chen^{1,2,*}, Atsushi Hosaka^{2,†}, Hiroshi Toki^{2,‡} and Shi-Lin Zhu^{1§}

¹*Department of Physics and State Key Laboratory of Nuclear Physics and Technology, Peking University, Beijing 100871, China*

²*Research Center for Nuclear Physics, Osaka University, Ibaraki, Osaka 567-0047, Japan*

The light scalar meson $\sigma(600)$ is known to appear at low excitation energy with very large width on top of continuum states. We investigate it in the QCD sum rule as an example of resonance structures appearing above the corresponding thresholds. We use all the possible local tetraquark currents by taking linear combinations of five independent local ones. We ought to consider the π - π continuum contribution in the phenomenological side of the QCD sum rule in order to obtain a good sum rule signal. We study the stability of the extracted mass against the Borel mass and the threshold value and find the $\sigma(600)$ mass at $530 \text{ MeV} \pm 40 \text{ MeV}$. In addition we find the extracted mass has an increasing tendency with the Borel mass, which is interpreted as caused by the width of the resonance.

PACS numbers: 12.39.Mk, 12.38.Lg, 12.40.Yx

Keywords: scalar meson, tetraquark, QCD sum rule

I. INTRODUCTION

The light scalar mesons, $\sigma(600)$, $\kappa(800)$, $f_0(980)$ and $a_0(980)$, have been intensively discussed for many years [1–3]. However, their nature is still not fully understood [4–8]. They have the same quantum numbers $J^{PC} = 0^{++}$ as the vacuum, and hence the structure of these states is a very important subject in order to understand non-perturbative properties of the QCD vacuum such as spontaneous chiral symmetry breaking. They compose of the flavor $SU(3)$ nonet with the mass below 1 GeV, and have a mass ordering which is difficult to be explained by using a $q\bar{q}$ configuration in the conventional quark model [9–13]. Therefore, several different pictures have been proposed, such as tetraquark states and meson-meson bound states, etc. Here we note that hadrons with complex structures such as tetraquarks may exist in the continuum above the threshold energy of two hadrons with simple quark structure.

The tetraquark structure of the scalar mesons was proposed long time ago by Jaffe with an assumption of strong diquark correlations [14, 15]. It can naturally explain their mass ordering and decay properties [16–18]. Yet the basic assumption of diquark correlation is not fully established. In this letter, we study $\sigma(600)$ as a tetraquark state in the QCD sum rule approach as an example of resonances in the continuum states above the π - π threshold. In the QCD sum rule, we calculate matrix elements from the QCD (OPE) and relate them to observables by using dispersion relations. Under suitable assumptions, the QCD sum rule has proven to be a very powerful and successful non-perturbative method in the past decades [19, 20]. Recently, this method has been applied to the study of tetraquarks by many authors [21–24].

In our previous paper [24], we have found that the QCD sum rule analysis with tetraquark currents implies the masses of scalar mesons in the region of 600 – 1000 MeV with the ordering $m_\sigma < m_\kappa < m_{f_0, a_0}$, while the conventional $\bar{q}q$ current is considerably heavier (larger than 1 GeV). To get this result, first we find there are five independent local tetraquark currents, and then we use one of these currents or linear combinations of two currents to perform the QCD sum rule analysis. But these interpolating currents do not describe the full space of tetraquark currents. In order to complete our previous study, we use more general currents by taking linear combinations of all these currents. It describes the full space of local tetraquark currents which can couple to $\sigma(600)$. Since $\sigma(600)$ meson is closely related to the π - π continuum and it has a wide decay width, we also consider the contribution of the π - π continuum as well as the effect of the finite decay width.

This paper is organized as follows. In Sec. II, we establish five independent local tetraquark currents, and perform a QCD sum rule analysis by using linear combinations of five single currents. In Sec. III, we perform a numerical analysis, and we also study the contribution of π - π continuum. In Sec. IV, we consider the effect of the finite decay width. Sec. V is devoted to summary.

*Electronic address: chx@water.pku.edu.cn

†Electronic address: hosaka@rcnp.osaka-u.ac.jp

‡Electronic address: toki@rcnp.osaka-u.ac.jp

§Electronic address: zhusl@pku.edu.cn

II. QCD SUM RULE

The local tetraquark currents for $\sigma(600)$ have been worked out in Ref [24]. There are two types of currents: diquark-antidiquark currents $(qq)(\bar{q}\bar{q})$ and meson-meson currents $(\bar{q}q)(\bar{q}q)$. These two constructions can be proved to be equivalent, and they can both describe the full space of local tetraquark currents [24]. Therefore we shall just use the first ones. Since we use their linear combinations to perform the QCD sum rule analysis, we can not distinguish whether it is a diquark-antidiquark state or a meson-meson bound state. However, we find that tetraquark currents with a single term do not lead to a reliable QCD sum rule result which means that $\sigma(600)$ probably has a complicated structure. The five independent local currents are given by:

$$\begin{aligned}
S_3^\sigma &= (u_a^T C \gamma_5 d_b)(\bar{u}_a \gamma_5 C \bar{d}_b^T - \bar{u}_b \gamma_5 C \bar{d}_a^T), \\
V_3^\sigma &= (u_a^T C \gamma_\mu \gamma_5 d_b)(\bar{u}_a \gamma^\mu \gamma_5 C \bar{d}_b^T - \bar{u}_b \gamma^\mu \gamma_5 C \bar{d}_a^T), \\
T_6^\sigma &= (u_a^T C \sigma_{\mu\nu} d_b)(\bar{u}_a \sigma^{\mu\nu} C \bar{d}_b^T + \bar{u}_b \sigma^{\mu\nu} C \bar{d}_a^T), \\
A_6^\sigma &= (u_a^T C \gamma_\mu d_b)(\bar{u}_a \gamma^\mu C \bar{d}_b^T + \bar{u}_b \gamma^\mu C \bar{d}_a^T), \\
P_3^\sigma &= (u_a^T C d_b)(\bar{u}_a C \bar{d}_b^T - \bar{u}_b C \bar{d}_a^T).
\end{aligned} \tag{1}$$

The summation is taken over repeated indices (μ, ν, \dots for Dirac, and a, b, \dots for color indices). The currents S, V, T, A and P are constructed by scalar, vector, tensor, axial-vector, pseudoscalar diquark and antidiquark fields, respectively. The subscripts 3 and 6 show that the diquarks (antidiquarks) are combined into the color representations, $\mathbf{3}_c$ and $\mathbf{6}_c$ ($\mathbf{3}_c$ and $\mathbf{6}_c$), respectively.

These five diquark-antidiquark currents $(qq)(\bar{q}\bar{q})$ are independent. In this work we use general currents by taking linear combinations of these five currents:

$$\eta = t_1 e^{i\theta_1} S_3^\sigma + t_2 e^{i\theta_2} V_3^\sigma + t_3 e^{i\theta_3} T_6^\sigma + t_4 e^{i\theta_4} A_6^\sigma + t_5 e^{i\theta_5} P_3^\sigma, \tag{2}$$

where t_i and θ_i are ten mixing parameters, whose linear combination describes the full space of local currents which can couple to $\sigma(600)$. We can not determine them in advance and therefore we choose them randomly for the study of the QCD sum rule.

By using the current in Eq. (2), we calculate the OPE up to dimension eight. To simplify our calculation, we neglect several condensates, such as $\langle g^3 G^3 \rangle$, etc., and we do not consider the α_s correction, such as $g^2 \langle \bar{q}q \rangle^2$, etc. The obtained OPE are shown in the following. We find that most of the crossing terms are not important such as ρ_{13} , and even more some of them disappear: $\rho_{15} = 0$, etc. For the most cases, we find that the OPE terms of Dim=6 and Dim=8 give major contributions in the OPE series in our region of interest. This is because the condensates $\langle \bar{q}q \rangle^2$ (D=6) and $\langle \bar{q}q \rangle \langle g \bar{q} \sigma G q \rangle$ (D=8) are much larger than others.

Since the OPE series should be convergent to give a reliable QCD sum rule, we also calculate the OPE of Dim=10 and Dim=12. However, we find that these terms are not important. Using the parameter set (2) and the the values of the condensates of the next section as an example, we show the convergence of the two-point correlation function $\Pi(M_B, s_0) \equiv \int_0^{s_0} \rho(s) e^{-s/M_B^2} ds$ in Fig. 1 as functions of M_B^2 . The threshold value is taken to be $s_0 = 1 \text{ GeV}^2$, and we show its behavior up to certain dimensions. We find that the OPE up to Dim=0 and Dim=2 are very small; the OPE of Dim=4 gives a minor contribution; the OPE of Dim=6 and Dim=8 are both important; the OPE of Dim=10 and Dim=12 are both small, and so we shall neglect them in the following analysis.

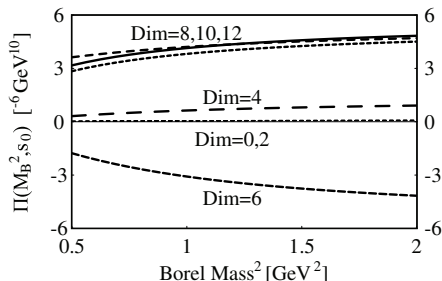


FIG. 1: The convergence of the two-point correlation function $\Pi(M_B, s_0)$. The threshold value is taken to be $s_0 = 1 \text{ GeV}^2$, and we show its behavior up to certain dimensions, as functions of M_B^2 . The solid line is for $\Pi(M_B, s_0)$ up to Dim=8. The short-dashed line around it is for $\Pi(M_B, s_0)$ up to Dim=10, and the long-dashed line around it is for $\Pi(M_B, s_0)$ up to Dim=12.

$$\begin{aligned}
\rho(s) = & t_1^2 \rho_{11}(s) + t_2^2 \rho_{22}(s) + t_3^2 \rho_{33}(s) + t_4^2 \rho_{44}(s) + t_5^2 \rho_{55}(s) \\
& + 2t_1 t_2 \cos(\theta_1 - \theta_2) \rho_{12}(s) + 2t_1 t_3 \cos(\theta_1 - \theta_3) \rho_{13}(s) + 2t_1 t_4 \cos(\theta_1 - \theta_4) \rho_{14}(s) \\
& + 2t_2 t_3 \cos(\theta_2 - \theta_3) \rho_{23}(s) + 2t_2 t_4 \cos(\theta_2 - \theta_4) \rho_{24}(s) + 2t_2 t_5 \cos(\theta_2 - \theta_5) \rho_{25}(s) \\
& + 2t_3 t_4 \cos(\theta_3 - \theta_4) \rho_{34}(s) + 2t_3 t_5 \cos(\theta_3 - \theta_5) \rho_{35}(s),
\end{aligned} \tag{3}$$

where

$$\begin{aligned}
\rho_{11}(s) = & \frac{s^4}{61440\pi^6} + \left(-\frac{m_u^2}{1536\pi^6} + \frac{m_u m_d}{1536\pi^6} - \frac{m_d^2}{1536\pi^6}\right) s^3 + \left(\frac{\langle g^2 GG \rangle}{6144\pi^6} - \frac{m_u \langle \bar{q}q \rangle}{192\pi^4} - \frac{m_d \langle \bar{q}q \rangle}{192\pi^4}\right) s^2 \\
& + \left(-\frac{m_u^2 \langle g^2 GG \rangle}{1024\pi^6} + \frac{m_u m_d \langle g^2 GG \rangle}{1024\pi^6} - \frac{m_d^2 \langle g^2 GG \rangle}{1024\pi^6} - \frac{m_u \langle g\bar{q}\sigma Gq \rangle}{64\pi^4} - \frac{m_d \langle g\bar{q}\sigma Gq \rangle}{64\pi^4} + \frac{\langle \bar{q}q \rangle^2}{12\pi^2}\right) s \\
& - \frac{7m_u^2 \langle \bar{q}q \rangle^2}{48\pi^2} + \frac{m_u m_d \langle \bar{q}q \rangle^2}{4\pi^2} - \frac{7m_d^2 \langle \bar{q}q \rangle^2}{48\pi^2} - \frac{m_u \langle g^2 GG \rangle \langle \bar{q}q \rangle}{768\pi^4} - \frac{m_d \langle g^2 GG \rangle \langle \bar{q}q \rangle}{768\pi^4} + \frac{\langle \bar{q}q \rangle \langle g\bar{q}\sigma Gq \rangle}{12\pi^2},
\end{aligned} \tag{4}$$

$$\rho_{22}(s) = \frac{s^4}{15360\pi^6} + \left(-\frac{m_u^2}{384\pi^6} - \frac{m_u m_d}{768\pi^6} - \frac{m_d^2}{384\pi^6}\right) s^3 + \left(\frac{\langle g^2 GG \rangle}{3072\pi^6} + \frac{m_u \langle \bar{q}q \rangle}{24\pi^4} + \frac{m_d \langle \bar{q}q \rangle}{24\pi^4}\right) s^2 \tag{5}$$

$$\begin{aligned}
& + \left(-\frac{m_u^2 \langle g^2 GG \rangle}{512\pi^6} + \frac{m_u m_d \langle g^2 GG \rangle}{512\pi^6} - \frac{m_d^2 \langle g^2 GG \rangle}{512\pi^6} + \frac{m_u \langle g\bar{q}\sigma Gq \rangle}{32\pi^4} + \frac{m_d \langle g\bar{q}\sigma Gq \rangle}{32\pi^4} - \frac{\langle \bar{q}q \rangle^2}{6\pi^2}\right) s \\
& + \frac{11m_u^2 \langle \bar{q}q \rangle^2}{12\pi^2} + \frac{2m_u m_d \langle \bar{q}q \rangle^2}{\pi^2} + \frac{11m_d^2 \langle \bar{q}q \rangle^2}{12\pi^2} - \frac{m_u \langle g^2 GG \rangle \langle \bar{q}q \rangle}{384\pi^4} - \frac{m_d \langle g^2 GG \rangle \langle \bar{q}q \rangle}{384\pi^4} - \frac{\langle \bar{q}q \rangle \langle g\bar{q}\sigma Gq \rangle}{6\pi^2},
\end{aligned} \tag{6}$$

$$\rho_{33}(s) = \frac{s^4}{1280\pi^6} + \left(-\frac{m_u^2}{32\pi^6} - \frac{m_d^2}{32\pi^6}\right) s^3 + \left(\frac{11\langle g^2 GG \rangle}{768\pi^6} + \frac{m_u \langle \bar{q}q \rangle}{4\pi^4} + \frac{m_d \langle \bar{q}q \rangle}{4\pi^4}\right) s^2 \tag{7}$$

$$\begin{aligned}
& + \left(-\frac{11m_u^2 \langle g^2 GG \rangle}{128\pi^6} - \frac{11m_d^2 \langle g^2 GG \rangle}{128\pi^6}\right) s \\
& + \frac{5m_u^2 \langle \bar{q}q \rangle^2}{\pi^2} + \frac{20m_u m_d \langle \bar{q}q \rangle^2}{\pi^2} + \frac{5m_d^2 \langle \bar{q}q \rangle^2}{\pi^2} + \frac{11m_u \langle g^2 GG \rangle \langle \bar{q}q \rangle}{96\pi^4} + \frac{11m_d \langle g^2 GG \rangle \langle \bar{q}q \rangle}{96\pi^4},
\end{aligned}$$

$$\rho_{44}(s) = \frac{s^4}{7680\pi^6} + \left(-\frac{m_u^2}{192\pi^6} + \frac{m_u m_d}{384\pi^6} - \frac{m_d^2}{192\pi^6}\right) s^3 + \frac{5\langle g^2 GG \rangle}{3072\pi^6} s^2 \tag{8}$$

$$\begin{aligned}
& + \left(-\frac{5m_u^2 \langle g^2 GG \rangle}{512\pi^6} + \frac{5m_u m_d \langle g^2 GG \rangle}{512\pi^6} - \frac{5m_d^2 \langle g^2 GG \rangle}{512\pi^6} - \frac{m_u \langle g\bar{q}\sigma Gq \rangle}{16\pi^4} - \frac{m_d \langle g\bar{q}\sigma Gq \rangle}{16\pi^4} + \frac{\langle \bar{q}q \rangle^2}{3\pi^2}\right) s \\
& - \frac{m_u^2 \langle \bar{q}q \rangle^2}{6\pi^2} + \frac{8m_u m_d \langle \bar{q}q \rangle^2}{3\pi^2} - \frac{m_d^2 \langle \bar{q}q \rangle^2}{6\pi^2} + \frac{m_u \langle g^2 GG \rangle \langle \bar{q}q \rangle}{128\pi^4} + \frac{m_d \langle g^2 GG \rangle \langle \bar{q}q \rangle}{128\pi^4} + \frac{\langle \bar{q}q \rangle \langle g\bar{q}\sigma Gq \rangle}{3\pi^2},
\end{aligned} \tag{9}$$

$$\rho_{55}(s) = \frac{s^4}{61440\pi^6} + \left(-\frac{m_u^2}{1536\pi^6} - \frac{m_u m_d}{1536\pi^6} - \frac{m_d^2}{1536\pi^6}\right) s^3 + \left(\frac{\langle g^2 GG \rangle}{6144\pi^6} + \frac{m_u \langle \bar{q}q \rangle}{64\pi^4} + \frac{m_d \langle \bar{q}q \rangle}{64\pi^4}\right) s^2 \tag{10}$$

$$\begin{aligned}
& + \left(-\frac{m_u^2 \langle g^2 GG \rangle}{1024\pi^6} - \frac{m_u m_d \langle g^2 GG \rangle}{1024\pi^6} - \frac{m_d^2 \langle g^2 GG \rangle}{1024\pi^6} + \frac{m_u \langle g\bar{q}\sigma Gq \rangle}{64\pi^4} + \frac{m_d \langle g\bar{q}\sigma Gq \rangle}{64\pi^4} - \frac{\langle \bar{q}q \rangle^2}{12\pi^2}\right) s \\
& + \frac{17m_u^2 \langle \bar{q}q \rangle^2}{48\pi^2} + \frac{7m_u m_d \langle \bar{q}q \rangle^2}{12\pi^2} + \frac{17m_d^2 \langle \bar{q}q \rangle^2}{48\pi^2} + \frac{m_u \langle g^2 GG \rangle \langle \bar{q}q \rangle}{256\pi^4} + \frac{m_d \langle g^2 GG \rangle \langle \bar{q}q \rangle}{256\pi^4} - \frac{\langle \bar{q}q \rangle \langle g\bar{q}\sigma Gq \rangle}{12\pi^2},
\end{aligned} \tag{11}$$

$$\rho_{12}(s) = \left(\frac{m_u^2}{3072\pi^6} + \frac{m_u m_d}{1536\pi^6} + \frac{m_d^2}{3072\pi^6}\right) s^3 + \left(-\frac{m_u \langle \bar{q}q \rangle}{48\pi^4} - \frac{m_d \langle \bar{q}q \rangle}{48\pi^4}\right) s^2 \tag{12}$$

$$\begin{aligned}
& + \left(-\frac{m_u \langle g\bar{q}\sigma Gq \rangle}{32\pi^4} - \frac{m_d \langle g\bar{q}\sigma Gq \rangle}{32\pi^4} + \frac{\langle \bar{q}q \rangle^2}{6\pi^2}\right) s - \frac{5m_u^2 \langle \bar{q}q \rangle^2}{12\pi^2} - \frac{m_u m_d \langle \bar{q}q \rangle^2}{2\pi^2} - \frac{5m_d^2 \langle \bar{q}q \rangle^2}{12\pi^2} + \frac{\langle \bar{q}q \rangle \langle g\bar{q}\sigma Gq \rangle}{6\pi^2},
\end{aligned}$$

$$\rho_{13}(s) = -\frac{\langle g^2 GG \rangle}{1024\pi^6} s^2 + \left(\frac{3m_u^2 \langle g^2 GG \rangle}{512\pi^6} + \frac{3m_d^2 \langle g^2 GG \rangle}{512\pi^6}\right) s - \frac{m_u \langle g^2 GG \rangle \langle \bar{q}q \rangle}{128\pi^4} - \frac{m_d \langle g^2 GG \rangle \langle \bar{q}q \rangle}{128\pi^4}, \tag{13}$$

$$\rho_{14}(s) = \left(\frac{3m_u^2 \langle g^2 GG \rangle}{4096\pi^6} + \frac{3m_u m_d \langle g^2 GG \rangle}{2048\pi^6} + \frac{3m_d^2 \langle g^2 GG \rangle}{4096\pi^6}\right) s - \frac{m_u \langle g^2 GG \rangle \langle \bar{q}q \rangle}{128\pi^4} - \frac{m_d \langle g^2 GG \rangle \langle \bar{q}q \rangle}{128\pi^4}, \tag{14}$$

$$\rho_{23}(s) = \left(-\frac{9m_u^2\langle g^2GG\rangle}{2048\pi^6} - \frac{9m_um_d\langle g^2GG\rangle}{1024\pi^6} - \frac{9m_d^2\langle g^2GG\rangle}{2048\pi^6}\right)_s + \frac{3m_u\langle g^2GG\rangle\langle\bar{q}q\rangle}{64\pi^4} + \frac{3m_d\langle g^2GG\rangle\langle\bar{q}q\rangle}{64\pi^4}, \quad (15)$$

$$\rho_{24}(s) = \frac{\langle g^2GG\rangle}{1024\pi^6}s^2 + \left(-\frac{3m_u^2\langle g^2GG\rangle}{512\pi^6} - \frac{3m_d^2\langle g^2GG\rangle}{512\pi^6}\right)_s + \frac{m_u\langle g^2GG\rangle\langle\bar{q}q\rangle}{128\pi^4} + \frac{m_d\langle g^2GG\rangle\langle\bar{q}q\rangle}{128\pi^4}, \quad (16)$$

$$\rho_{25}(s) = \left(\frac{m_u^2\langle g^2GG\rangle}{4096\pi^6} + \frac{m_um_d\langle g^2GG\rangle}{2048\pi^6} + \frac{m_d^2\langle g^2GG\rangle}{4096\pi^6}\right)_s - \frac{m_u\langle g^2GG\rangle\langle\bar{q}q\rangle}{384\pi^4} - \frac{m_d\langle g^2GG\rangle\langle\bar{q}q\rangle}{384\pi^4}, \quad (17)$$

$$\begin{aligned} \rho_{34}(s) = & \left(-\frac{m_u^2}{256\pi^6} - \frac{m_um_d}{128\pi^6} - \frac{m_d^2}{256\pi^6}\right)s^3 + \left(\frac{m_u\langle\bar{q}q\rangle}{4\pi^4} + \frac{m_d\langle\bar{q}q\rangle}{4\pi^4}\right)s^2 \\ & + \left(-\frac{15m_u^2\langle g^2GG\rangle}{2048\pi^6} - \frac{15m_um_d\langle g^2GG\rangle}{1024\pi^6} - \frac{15m_d^2\langle g^2GG\rangle}{2048\pi^6} + \frac{3m_u\langle g\bar{q}\sigma Gq\rangle}{8\pi^4} + \frac{3m_d\langle g\bar{q}\sigma Gq\rangle}{8\pi^4} - \frac{2\langle\bar{q}q\rangle^2}{\pi^2}\right)s \\ & + \frac{5m_u^2\langle\bar{q}q\rangle^2}{\pi^2} + \frac{6m_um_d\langle\bar{q}q\rangle^2}{\pi^2} + \frac{5m_d^2\langle\bar{q}q\rangle^2}{\pi^2} + \frac{5m_u\langle g^2GG\rangle\langle\bar{q}q\rangle}{64\pi^4} + \frac{5m_d\langle g^2GG\rangle\langle\bar{q}q\rangle}{64\pi^4} - \frac{2\langle\bar{q}q\rangle\langle g\bar{q}\sigma Gq\rangle}{\pi^2}, \end{aligned} \quad (18)$$

$$\rho_{35}(s) = -\frac{\langle g^2GG\rangle}{1024\pi^6}s^2 + \left(\frac{3m_u^2\langle g^2GG\rangle}{512\pi^6} + \frac{3m_d^2\langle g^2GG\rangle}{512\pi^6}\right)_s - \frac{m_u\langle g^2GG\rangle\langle\bar{q}q\rangle}{128\pi^4} - \frac{m_d\langle g^2GG\rangle\langle\bar{q}q\rangle}{128\pi^4}. \quad (19)$$

III. NUMERICAL ANALYSIS

To perform the numerical analysis, we use the values for all the condensates from Refs. [25–30]:

$$\begin{aligned} \langle\bar{q}q\rangle &= -(0.240 \text{ GeV})^3, \\ \langle\bar{s}s\rangle &= -(0.8 \pm 0.1) \times (0.240 \text{ GeV})^3, \\ \langle g_s^2GG\rangle &= (0.48 \pm 0.14) \text{ GeV}^4, \\ m_u &= 5.3 \text{ MeV}, m_d = 9.4 \text{ MeV}, \\ m_s(1 \text{ GeV}) &= 125 \pm 20 \text{ MeV}, \\ \langle g_s\bar{q}\sigma Gq\rangle &= -M_0^2 \times \langle\bar{q}q\rangle, \\ M_0^2 &= (0.8 \pm 0.2) \text{ GeV}^2. \end{aligned} \quad (20)$$

As usual we assume the vacuum saturation for higher dimensional operators such as $\langle 0|\bar{q}q\bar{q}q|0\rangle \sim \langle 0|\bar{q}q|0\rangle\langle 0|\bar{q}q|0\rangle$. There is a minus sign in the definition of the mixed condensate $\langle g_s\bar{q}\sigma Gq\rangle$, which is different with some other QCD sum rule calculation. This is just because the definition of coupling constant g_s is different [25, 31].

Altogether we took randomly chosen 50 sets of t_i and θ_i . Some of these sets of numbers lead to negative spectral densities in the low energy region of interest, which should be, however, positive from their definition. This is due to several reasons. One reason is that the convergence of OPE may not be achieved yet for those currents for the tetraquark state. Another reason is that some currents may not couple to the physical states properly. Except them, there are fifteen sets which lead to positive spectral densities. We show these fifteen sets of t_i and θ_i in Table I, and label them as (01), (02), \dots , (15). They are sorted by the fourth column ‘‘Pole Contribution’’ (PC):

$$\text{Pole Contribution} \equiv \frac{\int_0^{s_0} e^{-s/M_B^2} \rho(s) ds}{\int_0^\infty e^{-s/M_B^2} \rho(s) ds}. \quad (21)$$

The pole contribution (PC) is an important quantity to check the validity of the QCD sum rule analysis. Here, $\rho(s)$ denotes the spectral function. It depends on the ten mixed parameters as well as M_B and s_0 . We note that π - π continuum which we shall study later is not included in the pole contribution. By fixing $s_0 = 1 \text{ GeV}^2$, we show the PC values in Table I for the fifteen sets. ‘‘PC(0.5)’’, ‘‘PC(0.8)’’ and ‘‘PC(1.2)’’ denote pole contribution by setting $M_B^2 = 0.5 \text{ GeV}^2$, 0.8 GeV^2 and 1.2 GeV^2 , respectively. We find that the pole contribution decreases very rapidly as the Borel Mass increases. Since we have discussed the convergence of OPE in the previous section, and found that the Dim=10 and Dim=12 terms are much smaller than the Dim=6 and Dim=8 terms, and so it is only the pole contribution which gives a upper limitation on the Borel Mass. The Borel window is wider for the former parameter sets (1), (2), \dots , and narrower for the latter ones. It almost disappears for the set (15), whose mass prediction is

TABLE I: Values for parameters t_i , θ_i , the mass range M_σ , the pole contribution (PC) and the continuum amplitude $a(t_i, \theta_i)$. The meaning of these quantities are given in the text. There are altogether fifteen sets, which are sorted by the fourth column ‘‘PC’’. ‘‘PC(0.5)’’, ‘‘PC(0.8)’’ and ‘‘PC(1.2)’’ denote pole contribution by setting $M_B^2 = 0.5 \text{ GeV}^2$, 0.8 GeV^2 and 1.2 GeV^2 , respectively.

No	t_1	t_2	t_3	t_4	t_5	θ_1	θ_2	θ_3	θ_4	θ_5	$M_\sigma(\text{MeV})$	PC(0.5)	PC(0.8)	PC(1.2)	a (GeV^4)
(1)	0.03	0.03	0.73	0.37	0.24	2.7	3.4	4.7	5.5	3.6	510 ~ 580	92%	52%	13%	1.2×10^{-7}
(2)	0.03	0.92	0.75	0.70	0.03	5.6	0.80	4.1	2.9	2.5	510 ~ 590	90%	46%	11%	5.5×10^{-7}
(3)	0.25	0.79	0.16	0.95	0.22	1.8	1.2	6.1	0.44	1.8	510 ~ 600	87%	44%	11%	3.6×10^{-7}
(4)	0.53	0.26	0.93	0.24	0.76	2.9	0.40	2.0	2.5	3.3	510 ~ 610	85%	41%	10%	1.7×10^{-6}
(5)	0.74	0.54	0.74	0.65	0.67	0.15	3.1	1.4	2.7	6.1	520 ~ 640	81%	36%	8%	1.9×10^{-6}
(6)	0.98	0.50	0.12	0.33	0.03	2.0	4.0	6.3	1.3	1.6	510 ~ 590	82%	32%	6%	5.8×10^{-8}
(7)	0.98	0.42	0.84	0.82	0.72	0.095	1.5	3.7	2.4	3.0	540 ~ 700	70%	26%	6%	4.2×10^{-6}
(8)	0.48	0.68	0.58	0.96	0.04	1.8	2.5	3.0	4.3	3.7	530 ~ 690	70%	25%	6%	1.9×10^{-6}
(9)	0.53	1.0	0.99	0.34	0.86	5.6	4.8	5.3	4.1	0.076	540 ~ 700	68%	24%	5%	4.5×10^{-6}
(10)	0.75	0.96	0.32	0.12	0.11	4.3	2.6	0.93	5.1	2.9	560 ~ 760	57%	17%	4%	9.5×10^{-7}
(11)	0.31	0.81	0.71	0	0.10	4.2	1.8	2.8	5.4	5.1	570 ~ 780	55%	17%	4%	3.2×10^{-6}
(12)	0.47	0.40	0	0.46	0.91	0.18	1.9	1.9	0.091	0.94	540 ~ 730	58%	16%	3%	2.0×10^{-7}
(13)	0.60	0.26	0.44	0.27	0.24	3.3	3.6	0.92	5.9	3.7	620 ~ 850	43%	13%	3%	1.7×10^{-6}
(14)	0.74	0.73	0.73	0.32	0.28	1.3	1.3	4.6	3.3	5.6	620 ~ 850	42%	12%	3%	4.3×10^{-6}
(15)	0.65	0.55	0.92	0.19	0.96	4.9	5.2	4.0	5.5	3.3	730 ~ 930	25%	7%	2%	5.4×10^{-6}

also much different from others. The Borel window should be our working region. However, since the Borel stability is always very good when $M_B^2 > 0.5 \text{ GeV}^2$, we shall keep the idea of Borel window in mind and work in the region $0.5 < M_B^2 < 2 \text{ GeV}^2$. On the other side, we shall care more about the threshold value s_0 .

By using these fifteen sets of numbers, we perform the QCD sum rule analysis. There are two parameters, the Borel mass M_B and the threshold value s_0 in the QCD sum rule analysis. We find that the Borel mass stability is usually good, but the threshold value stability is not always good. We show the mass range of $\sigma(600)$, M_σ , in Table I, where the working region is taken to be $0.8 \text{ GeV}^2 < s_0 < 1.2 \text{ GeV}^2$ and $0.8 \text{ GeV}^2 < M_B^2 < 2 \text{ GeV}^2$. We find the mass range is small when the pole contribution (PC) is large.

The parameter sets (01)-(06) lead to relatively good threshold value stability. Taking the set (02) as an example, we show its spectral density $\rho(s)$ in Fig 2 as function of s . It is positive definite, and has a small value around $s \sim 1.2 \text{ GeV}^2$. Therefore, the threshold value dependence is weak around this point, as shown in Fig. 3 for the extracted mass as functions of both M_B^2 and s_0 . We find all the curves are very stable in the region $0.5 \text{ GeV}^2 < M_B^2 < 2 \text{ GeV}^2$ and $0.6 \text{ GeV}^2 < s_0 < 1.4 \text{ GeV}^2$. From the set (02) we can extract the mass of $\sigma(600)$ around 550 MeV. From other good cases, we find that the mass of $\sigma(600)$ is around 550 MeV as well.

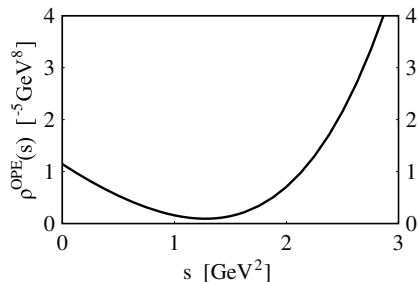


FIG. 2: The spectral density $\rho(s)$ calculated by the mixed current η , as a function of s . We show the results of the parameter set (02) as an example.

The parameter sets (07)-(15) lead to the threshold value stability, which is not good. Taking the set (13) as an example, we show its spectral density in Fig. 4 as a function of s (left figure), and the extracted mass in Fig. 5 as a function of s_0 (upper three curves). The mass increases with s_0 and we cannot extract the mass from this result. Many effects contribute to the mass dependence on the threshold value, but for $\sigma(600)$ the π - π continuum contribution is probably the dominant one. Hence, we add a term $\rho_{\pi\pi}(s)$ in the spectral function in the phenomenological side to

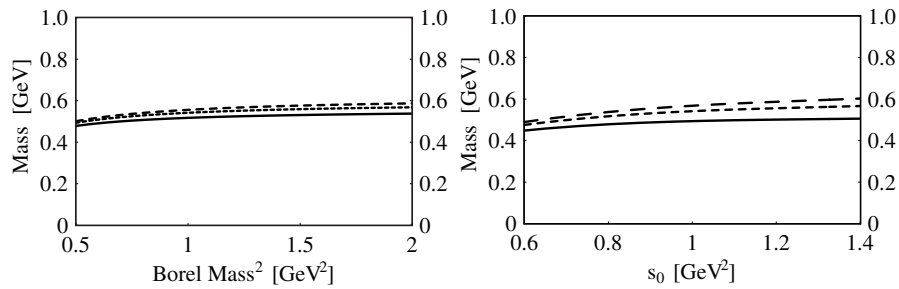


FIG. 3: The extracted mass of $\sigma(600)$ as a tetraquark state calculated by the mixed current η , as functions of the Borel mass M_B and the threshold value s_0 . We show the results of the parameter set (02) as an example. At the left panel, the solid, short-dashed and long-dashed curves are obtained by setting $s_0 = 0.8, 1$ and 1.2 GeV^2 , respectively. At the right panel, the solid and dashed curves are obtained by setting $M_B^2 = 0.5, 1$ and 2 GeV^2 , respectively.

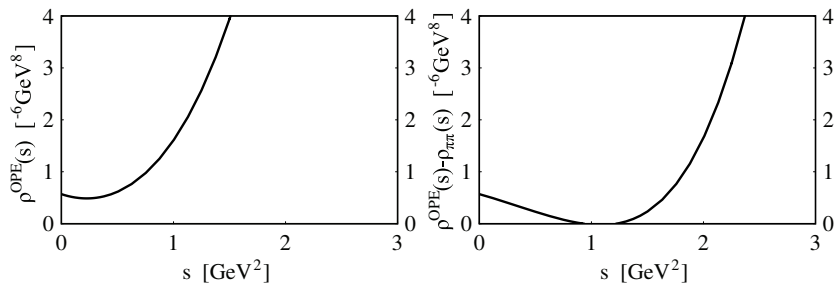


FIG. 4: The spectral density $\rho(s)$ calculated by the mixed current η , as a function of s . We show the results of the parameter set (13) as an example. The left figure shows the full spectral density as given on the left hand side of Eq. (22), while the right figure is the one with $\rho_{\pi\pi}(s)$ subtracted.

describe the π - π continuum:

$$\rho(s) = f_Y^2 \delta(s - M_Y^2) + \rho_{\pi\pi}(s) + \rho_{cont}. \quad (22)$$

where ρ_{cont} is the standard expression of the continuum contribution except the π - π continuum. To find an expression

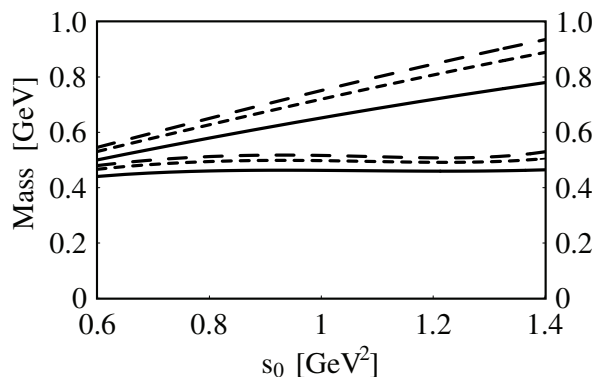


FIG. 5: The extracted mass of $\sigma(600)$ as a tetraquark state calculated by the mixed current η , as functions of the threshold value s_0 . We choose the parameter set (13) as an example. The solid, short-dashed and long-dashed curves are obtained by setting $M_B^2 = 0.5, 1$ and 2 GeV^2 , respectively. The upper three curves are obtained without adding the contribution of the π - π continuum in the phenomenological side, while the lower three curves are obtained after adding the contribution of the π - π continuum.

for $\rho_{\pi\pi}(s)$, we introduce a coupling

$$\lambda_{\pi\pi} \equiv \langle 0|\eta|\pi^+\pi^- \rangle. \quad (23)$$

The correlation function of the π - π continuum is

$$\Pi_{\pi\pi}(p^2) = i \int \frac{d^4q}{(2\pi)^2} \frac{i}{(p+q)^2 - m_\pi^2 + i\epsilon} \frac{i}{q^2 - m_\pi^2 + i\epsilon} |\lambda_{\pi\pi}|^2, \quad (24)$$

and the spectral density of the π - π continuum is just its imaginary part

$$\rho_{\pi\pi}(s) = \text{Im}\Pi_{\pi\pi}(s) = \frac{1}{16\pi^2} \sqrt{1 - \frac{4m_\pi^2}{s}} |\lambda_{\pi\pi}|^2. \quad (25)$$

We may calculate $\lambda_{\pi\pi}$ by using the method of current algebra if we know the property of the resonance state. However, this is not the topic of this paper. Moreover, in this paper we use a general local tetraquark current to test the full space of local tetraquark currents, so we again make some try and error tests, and find that the following function leads to a reasonable QCD sum rule result, $\lambda_{\pi\pi} \sim s$. Hence, we take the spectral density of the π - π continuum as

$$\rho_{\pi\pi}(s) = a(t_i, \theta_i) s^2 \sqrt{1 - \frac{4m_\pi^2}{s}}. \quad (26)$$

We add the continuum contribution $\rho_{\pi\pi}(s)$ in the phenomenological side and perform the QCD sum rule analysis. The values of parameter $a(t_i, \theta_i)$ are listed in Table I. After adding the continuum contribution, the threshold value stability becomes much better. Still taking the set (13) as an example, we show its spectral density in Fig. 4 as a function of s (right figure), and the extracted mass in Fig. 5 as functions of s_0 (lower three curves). We see that now the spectral density has a small value around $s \sim 1.1 \text{ GeV}^2$, and the stability of the threshold value is significantly improved.

Hence, we made the same analysis for all the other cases. We found all the cases are good except one, which is the case (15), where we are not able to get the desired stability as a function of s_0 . The mass function has a small stability region and increases rapidly with s_0 . Hence, we consider this case is between the good case and bad case, and remove it from the further analysis in this paper. We show several results out of all the good cases in Fig. 6, which are obtained by using the parameter sets (01), (03), (06), (09), (12) and (14). We list the used $a(t_i, \theta_i)$ in Table 1 for all the cases. All the masses behave very nicely as functions of the Borel mass and s_0 as shown in Fig. 6. In our working region $0.8 \text{ GeV}^2 < s_0 < 1.2 \text{ GeV}^2$ and $0.8 \text{ GeV}^2 < M_B^2 < 2 \text{ GeV}^2$, all the cases lead to a mass within the region $495 \text{ MeV} \sim 570 \text{ MeV}$. From this mass range, the mass of $\sigma(600)$ is extracted to be $530 \text{ MeV} \pm 40 \text{ MeV}$.

IV. THE EFFECT OF FINITE DECAY WIDTH

After the s_0 stability has been improved, we notice now that the mass increases systematically with the Borel mass as seen in Fig. 6 in all the cases. We therefore try to consider a possible reason of this systematic result. The $\sigma(600)$ meson has a large decay width. We parametrize it by a Gaussian distribution instead of the δ -function for the $\sigma(600)$.

$$\rho^{FDW}(s) = \frac{f_X^2}{\sqrt{2\pi}\sigma_X} \exp\left(-\frac{(\sqrt{s}-M_X)^2}{2\sigma_X^2}\right). \quad (27)$$

The Gaussian width σ_X is related to the Breit-Wigner decay width Γ by $\sigma_X = \Gamma/2.4$. We set $\sigma_X = 200 \text{ MeV}$, and $M_X = 550 \text{ MeV}$, and calculate the following ‘‘mass’’:

$$M^2(M_B, s_0) = \frac{\int_0^{s_0} e^{-s/M_B^2} s \exp\left(-\frac{(\sqrt{s}-M_X)^2}{2\sigma_X^2}\right) \frac{ds}{2\sqrt{s}}}{\int_0^{s_0} e^{-s/M_B^2} \exp\left(-\frac{(\sqrt{s}-M_X)^2}{2\sigma_X^2}\right) \frac{ds}{2\sqrt{s}}}. \quad (28)$$

We find that the obtained mass M is not just 550 MeV , but increases as M_B^2 increases as shown in Fig. 7. Hence, the extracted mass in the QCD sum rule analysis ought to depend on the Borel mass. The amount of the change of the extracted mass in the QCD sum rule analysis is similar to the one found in this model calculation. Moreover, we find that the finite decay width does not change the final result significantly, which we have also noticed in our previous paper [24].

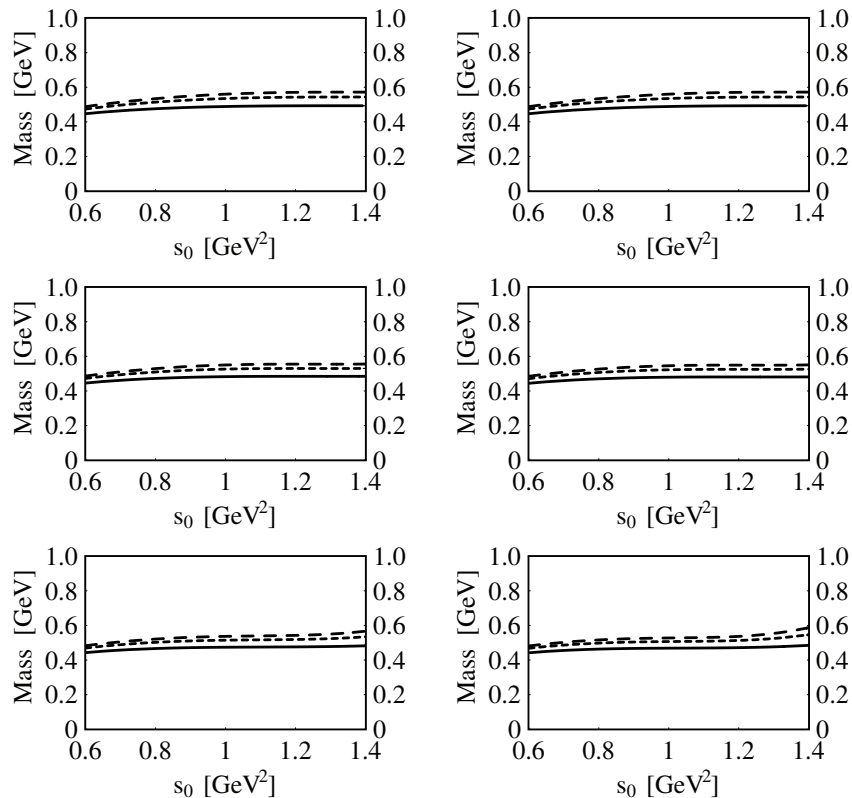


FIG. 6: The extracted mass of $\sigma(600)$ as a tetraquark state calculated by the mixed currents η , as functions of the threshold value s_0 . We choose the parameter sets (01), (03), (06), (09), (12) and (14). The results are shown in sequence. The solid, short-dashed and long-dashed curves are obtained by setting $M_B^2 = 0.5, 1$ and 2 GeV^2 , respectively.

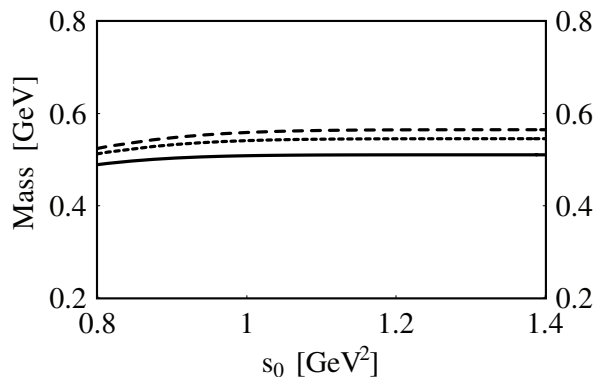


FIG. 7: The extracted “mass” considering a finite decay width. The solid, short-dashed and long-dashed curves are obtained by setting $M_B^2 = 0.5, 1$ and 2 GeV^2 , respectively.

V. SUMMARY

In summary, we have studied the light scalar meson $\sigma(600)$ in the QCD sum rule. We have used general local tetraquark currents which are linear combinations of five independent local ones. This describes the full space of local tetraquark currents which can couple to $\sigma(600)$ either strongly or weakly. We find some cases where the stability of the Borel mass and threshold value is both good, while in some cases the threshold value stability is not so good. The resonance mass has an increasing trend with s_0 , which indicates a continuum contribution. Hence, we have introduced a contribution from the π - π continuum, and obtained a good threshold value stability. The mass of $\sigma(600)$

is extracted to be $530 \text{ MeV} \pm 40 \text{ MeV}$. Very interesting observation is that the mass increases slightly with the Borel mass. We have made a model calculation by taking the Gaussian width of 200 MeV centered at 550 MeV and try to make a sum rule analysis. We see a similar increase trend as seen in the QCD sum rule analysis.

The continuum contribution exists in the background of the $\sigma(600)$ meson and it is very important to consider this fact in the QCD sum rule analysis for exotic states. We have seen clear tendency of the mass increase with the Borel mass after getting good signal of the threshold dependence. The decay width of $\sigma(600)$ is related to this increase tendency. We are now trying to calculate this by using the three-point correlation function within the QCD sum rule approach. The present analysis is very encouraging to apply the QCD sum rule including the continuum states for other scalar mesons. Moreover, the continuum contribution should be important in many other resonances such as $\Lambda(1405)$ etc, which lies in some continuum background. In the future, we will use the QCD sum rule analysis with continuum to study various resonances.

Acknowledgments

This project is supported by the National Natural Science Foundation of China under Grants No. 10625521 and No. 10721063, the Ministry of Science and Technology of China (2009CB825200), the Ministry of Education research Grant: Kakenhi (18540269), and the Grant for Scientific Research ((C) No. 19540297) from the Ministry of Education, Culture, Science and Technology, Japan.

-
- [1] C. Amsler and N. A. Tornqvist, Phys. Rept. **389**, 61 (2004).
 - [2] D. V. Bugg, Phys. Rept. **397**, 257 (2004).
 - [3] E. Klempt and A. Zaitsev, Phys. Rept. **454**, 1 (2007).
 - [4] I. Caprini, G. Colangelo and H. Leutwyler, Phys. Rev. Lett. **96**, 132001 (2006).
 - [5] T. Hatsuda and T. Kunihiro, Phys. Rept. **247**, 221 (1994).
 - [6] J. A. Oller and E. Oset, Nucl. Phys. A **620**, 438 (1997) [Erratum-ibid. A **652**, 407 (1999)].
 - [7] J. Sugiyama, T. Nakamura, N. Ishii, T. Nishikawa and M. Oka, Phys. Rev. D **76**, 114010 (2007).
 - [8] S. Prelovsek, T. Draper, C. B. Lang, M. Limmer, K. F. Liu, N. Mathur and D. Mohler, arXiv:1002.0193 [hep-ph].
 - [9] C. Amsler *et al.* [Particle Data Group], Phys. Lett. B **667**, 1 (2008).
 - [10] E. M. Aitala *et al.* [E791 Collaboration], Phys. Rev. Lett. **86**, 770 (2001).
 - [11] M. Ablikim *et al.* [BES Collaboration], Phys. Lett. B **598**, 149 (2004).
 - [12] D. Aston *et al.*, Nucl. Phys. B **296**, 493 (1988).
 - [13] R. R. Akhmetshin *et al.* [CMD-2 Collaboration], Phys. Lett. B **462**, 380 (1999).
 - [14] R. L. Jaffe, Phys. Rev. D **15**, 267 (1977).
 - [15] R. L. Jaffe, Phys. Rev. D **15**, 281 (1977).
 - [16] M. G. Alford and R. L. Jaffe, Nucl. Phys. B **578**, 367 (2000).
 - [17] L. Maiani, F. Piccinini, A. D. Polosa and V. Riquer, Phys. Rev. Lett. **93**, 212002 (2004).
 - [18] J. D. Weinstein and N. Isgur, Phys. Rev. D **41**, 2236 (1990).
 - [19] M. A. Shifman, A. I. Vainshtein and V. I. Zakharov, Nucl. Phys. B **147**, 385 (1979).
 - [20] L. J. Reinders, H. Rubinstein and S. Yazaki, Phys. Rept. **127**, 1 (1985).
 - [21] M. E. Bracco, A. Lozea, R. D. Matheus, F. S. Navarra and M. Nielsen, Phys. Lett. B **624**, 217 (2005).
 - [22] S. Narison, Phys. Rev. D **73**, 114024 (2006).
 - [23] H. J. Lee and N. I. Kochelev, Phys. Lett. B **642**, 358 (2006).
 - [24] H. X. Chen, A. Hosaka and S. L. Zhu, Phys. Rev. D **76**, 094025 (2007).
 - [25] K. C. Yang, W. Y. P. Hwang, E. M. Henley and L. S. Kisslinger, Phys. Rev. D **47**, 3001 (1993).
 - [26] S. Narison, Camb. Monogr. Part. Phys. Nucl. Phys. Cosmol. **17**, 1 (2002).
 - [27] V. Gimenez, V. Lubicz, F. Mescia, V. Porretti and J. Reyes, Eur. Phys. J. C **41**, 535 (2005).
 - [28] M. Jamin, Phys. Lett. B **538**, 71 (2002).
 - [29] B. L. Ioffe and K. N. Zyblyuk, Eur. Phys. J. C **27**, 229 (2003).
 - [30] A. A. Ovchinnikov and A. A. Pivovarov, Sov. J. Nucl. Phys. **48**, 721 (1988) [Yad. Fiz. **48**, 1135 (1988)].
 - [31] W. Y. P. Hwang and K. C. Yang, Phys. Rev. D **49**, 460 (1994).